Ancient TL

Short Communication

# Evaluating short-term post-irradiation instability of radiation-induced ESR signals in quartz

Eslem Ben Arous[1,2,3*], María Jesús Alonso Escarza[1], Verónica Guilarte[4], Sumiko Tsukamoto[5,6], Mathieu Duval[1,7,8]

[1]Centro Nacional de Investigación sobre la Evolución Humana (CENIEH), Burgos, Spain
[2]Human Palaeosystems Group, Max Planck Institute of Geoanthropology (MPI-GEA), Jena, Germany
[3]Histoire Naturelle des Humanités Préhistoriques (HNHP), CNRS–Université de Perpignan Via Domitia (UPVD)–Muséum national d'Histoire naturelle (MNHN), Paris, France
[4]Department of Science Education, University of Granada, Melilla, Spain
[5]LIAG-Institute for Applied Geophysics, Hannover, Germany
[6]Department of Geosciences, University of Tübingen, Tübingen, Germany
[7]Australian Research Centre for Human Evolution (ARCHE), Griffith University, Brisbane, Queensland, Australia
[8]Palaeoscience Labs, Department of Archaeology and History, La Trobe University Melbourne Campus, Bundoora, Victoria, Australia

*Corresponding author: ben-arous@gea.mpg.de

*Received: 03 October 2025; in final form: 26 November 2025; accepted: 26 November 2025*

## Abstract

**This study investigates the potential short-term fading of radiation-induced Electron Spin Resonance (ESR) signals in quartz grains following gamma-irradiation, a critical issue for the optimization of Single Aliquot (SA) measurement protocols. Through a signal stability experiment carried out on two quartz samples, we evaluated the evolution of the Al and Ti ESR signal intensities over 2 to 8 months after gamma irradiation. Our results indicate that the variation of the ESR intensities remains within typical experimental uncertainties, although data might also suggest a potential trend during the first day after irradiation. This trend is, however, non-systematic and could be sample- and signal-dependent, if not directly related to the stability of the experimental setup. Regardless, for precaution we may nevertheless recommend waiting for 1 day after gamma-irradiation before carrying out the ESR measurements. Importantly, this finding implies that ESR measurements of quartz samples can be performed relatively soon after gamma-irradiation, enabling the implementation of more time-efficient SAR protocols for ESR dating applications.**

**Keywords: Fading, ESR signal, Quartz, MAAD, SAR**

## 1. Introduction

Most Multiple Centre Electron Spin Resonance (MC-ESR) dating studies based on sedimentary quartz grains typically use the standard Multiple Aliquot Additive Dose (MAAD) method for dose determination (e.g. Ben Arous et al., 2025, 2024b; Duval et al., 2017; Liu et al., 2010; Voinchet et al., 2020; Yokoyama et al., 1985). More convenient in many aspects than Single Aliquot (SA) procedures, especially when direct access to an irradiation source may be complicated, the MAAD method has demonstrably proven its reliability to constrain the chronology of Quaternary deposits in Europe, Asia, and Africa, providing results in good agreement with independent age control (e.g., Bartz et al., 2018, 2019; Ben Arous et al., 2024b, 2025; Duval et al., 2022; Voinchet et al., 2020). However, one may reasonably argue that ESR dose evaluations involving Single Aliquot and/or Regeneration procedures (e.g., SAR,

SAAD, MAR) show indisputable advantages compared to the MAAD method. For example, SA measurements require a significantly smaller amount of prepared material, which may be critical in quartz-poor deposits. In combination with Regeneration (SAR), it also involves significantly less irradiation dose steps, significantly reducing irradiation and measurement times. Typically, only 3–4 dose points may be needed for the dose response curve, compared to 10–12 dose points usually measured for the MAAD. Moreover, the dose evaluation based on SAR or MAR methods intrinsically offers a smaller fitting uncertainty, since the $D_e$ is obtained by interpolation instead of back extrapolation. This is why the SAR has become an increasingly popular method in ESR dating over the last decade (e.g., Tsukamoto et al., 2015).

Time constraint being the essence of any experimental work, one of the main issues with regenerative dose measurement procedures is to properly evaluate whether any transient (short-lived) ESR signal induced by the irradiation may potentially interfere with the main radiation-induced ESR signals being measured for dating purposes. Such evaluation is crucial in order to determine the appropriate waiting time needed between the irradiation and subsequent ESR measurement. However, unlike for tooth enamel (e.g., Hoffmann and Mangini, 2002; IAEA, 2002; Nilsson et al., 2001; Sholom and Chumak, 2008), the possible presence of transient radiation-induced ESR signals in quartz grains remains virtually unknown to our knowledge.

Regardless of the above, two main conservative strategies have been traditionally adopted in ESR dating of quartz to mitigate the potential impact of transient signals on dose evaluation: (i) either a prolonged storage (which can vary from a few days to a few months depending on the material or laboratory involved) of the sample at room temperature (e.g. Fattibene and Callens, 2010), (ii) a post-irradiation annealing at a given temperature, regarded as sufficient to eliminate the temporary signals without affecting the radiation-induced signal of interest. This first one is usually favoured in dating application studies based on the MAAD method, and a minimum storage of a few weeks (the exact duration is very rarely reported) is commonly considered for extra precaution (e.g. Niu et al., 2022), although there is currently no published evidence that could possibly confirm, or invalidate, the need of such procedure. The second is usually preferred for SAR protocol measurement based on quartz (e.g. Tsukamoto et al., 2015). In simplified terms, to determine the equivalent dose with the SAR protocol, the natural ESR signal of a single aliquot is first measured after preheating at a specific temperature (typically between 120 °C and 280 °C for 2 min). This is followed by a high-temperature annealing step (420 °C for 2 min), irradiation with an X-ray source (given dose), another preheating step, and finally measurement of the regenerated ESR signal from the same aliquot. The ESR-SAR protocol offers the major advantage of saving considerable time, as it allows the quartz sample to be measured just a few minutes after irradiation and heating, unlike the MAAD protocol, where all irradiations are performed in a separate facility using a high dose rate source.

Consequently, the present study aims to evaluate the possible presence of transient radiation-induced ESR signals generated by gamma-irradiation, through a short-term stability experiment involving two quartz samples repeatedly measured over 2 and 8 months after irradiation. Such experiment is also crucial for the future implementation of the SAR protocol using gamma-irradiation sources.

## 2. Materials and methods

Two prepared quartz samples (100–200 µm grain size), OUC1102 and BG03-06, were selected for our experiment carried out at CENIEH (Spain). OUC1102 is a modern sample originating from the river bank of Oued Charef, Morocco (Ben Arous et al., 2024a; Sala-Ramos et al., 2022). BG03-06 was collected from the Middle Stone Age of Bargny 3 in Senegal (Ben Arous et al., 2024b). One natural aliquot of each sample (OUC1102: 304.6 mg; BG03-06: 150.9 mg) was irradiated with a Gammacell-1000 $^{137}$Cs gamma-source (OUC1102: 1327 Gy; BG03-06: 1000 Gy) and then measured by ESR. Low temperature (90–92 K) ESR measurements were performed with an EMXmicro 6/1Bruker X-band ESR spectrometer coupled to a standard rectangular ER 4102ST cavity and using an ER4141VT digital temperature control unit. To ensure constant experimental conditions over time, the temperature of the water circulating in the magnet was controlled and stabilized at 18 °C by a water-cooled Thermo Scientific NESLAB ThermoFlex 3500 chiller, and the temperature of the room was kept constant at 20 °C by an air conditioning unit. Further details about the setup and its stability over time can be found in Duval and Guilarte Moreno (2012) and Guilarte and Duval (2020).

The ESR signals of both the Al and Ti centres were measured separately using the following acquisition parameters:

- Al centre: 10 mW microwave power, 1024 points resolution, 20 mT sweep width, 100 kHz modulation frequency, 0.1 mT modulation amplitude, 40 ms conversion time, 10 ms time constant and 1 scan.
- Ti centres: 5 mW microwave power, 1024 points resolution, 20 mT sweep width, 100 kHz modulation frequency, 0.1 mT modulation amplitude, 60 ms conversion time,10 ms time constant and 1 to 3 scans.

Each aliquot of a given sample was measured 3 times after a $\sim 120\,^{\circ}$ rotation in the cavity for both Al and Ti signals in order to consider angular dependence of the signal due to sample heterogeneity, and a mean value and an associated standard deviation were derived. Another quartz sample was used as a standard and measured immediately before and after the aliquots to evaluate the stability of the experimental conditions over time. Repeated ESR measurements of each aliquot together with the standard were carried out over a period of 8 months after after gamma-irradiation for OUC1102, and over 2 months for BG03-06.

The ESR intensity of the Al signal was extracted from peak-to-peak amplitude measurements between the top of the

first peak and the bottom of the last peak in the domain ranging from $g = 2.0185$ to $g = 1.9928$ (Toyoda and Falguères, 2003). The ESR intensity of the Ti centres was evaluated by peak-to-baseline amplitude measurement around $g = 1.913$ to $g = 1.915$ (i.e., options C and D sensu Duval and Guilarte, 2015). All ESR intensities were corrected for the slight variations of temperature (up to $\sim 0.2$ K) following Duval and Guilarte Moreno (2012), and of the overall stability of the experimental setup using the values from the quartz standard as a reference.

## 3. Results

The results obtained for the two samples and for each signal (Al, Ti-H and Ti-mix) are summarised in Table 1 and Fig. 1, while the numerical data may be found in Supplementary Material Tables S1 and S2.

An apparent trend may be observed in the ESR intensity of the Al signal of OUC1102 during the first 5 hours (300 min; Fig. 1B), which decreases by about 5 % from 5.57 to 5.30 a.u. Then, the values increase again and oscillate between 5.34 and 5.67 a.u. (Fig. 1A). In contrast, the Al signal intensity of BG03-06 first drops by about 4 % from 2.11 to 2.02 a.u., and then shows a slight but constant increase during the first 5 hours of about 11 % (from 2.02 to 2.25 a.u.) (Fig. 1D). This trend seems to disappear after 1 day, and ESR intensities remain overall constant between 1.96 and 2.14 a.u. (Fig. 1C).

Unlike the Al signal, the Ti signals measured in OUC1102 do not show any obvious apparent trend during the first 5 hours or beyond (Fig. 1E and F). In contrast, the two Ti signals of BG03-06 do show a similar notable increase over the first 5 hours of about 21 % (Ti-H; from 0.23 to 0.28 a.u.) and 18 % (Ti-mix; from 0.33 to 0.39 a.u.) (Fig. 1G and H). After 1 day, the ESR intensities seem to show instead a more random variation (Ti-H : 0.24–0.28 a.u.; Ti-mix: 0.32–0.37 a.u) and no significant trend may be observed. Interestingly, the evolution of the Al and Ti signals of BG03-06 is similar, although the overall variability of the Al is lower than that of the Ti signals.

Despite the variability observed in the Al and Ti signal intensities, both samples show that the mean intensity value remains virtually unchanged regardless of the time range considered. For OUC1102, the mean ESR intensities of the Al signal are between 5.51 ± 0.10 a.u. (234 days) and 5.44 ± 0.09 a.u. (1 day) and remain systematically consistent within uncertainty (Table 1). Similarly, the mean ESR intensities of the Ti-H and Ti-mix in that sample remain around 0.19 a.u. and 0.28–0.29 a.u., respectively (Table 1). BG03-06 also show mean ESR intensities varying within narrow range between 2.09 ± 0.06 a.u. (64 days) and 2.13 ± 0.06 a.u. (21 days), $\sim$0.26–0.27 a.u. and $\sim$0.34–0.35 a.u. for the Al, Ti-H and Ti-mix signals, respectively (Table 1). In other words, despite the variability observed, no significant difference in the ESR intensities of the various signals can be observed 2 hours, 1 day, 7 days and 14 days after gamma-irradiation when compared to the baseline values collected over a longer period (234 days for OUC1102 and 64 days for BG03-06).

This variability most likely originates from the inherent uncertainty associated with the stability of the experimental setup (about 1.1 % and 2.8 % for the Al and Ti signals; Duval et al., 2024; Duval and Guilarte Moreno, 2012) or with sample homogeneity, and especially the angular dependence of the signal. The latter is typically about 1.1 %, 2.0 % and 3.0 % for the Al, Ti-mix and T-H signals, although higher values may also be observed (Duval et al., 2024). Moreover, the variability is also strongly dependent on the signal-to-noise ($S/N$) ratio associated to each signal. For example, for sample BG03-06 the mean $S/N$ ratio of the Al signal is about 2.1 and 5.4 times higher than that of the Ti-H and Ti-mix signals, respectively (Table 1). A similar observation can be made for sample OUC1102, with the Al signal showing an $S/N$ ratio approximately 5–16 times higher on average for the various successive measurements (Table 1). Interestingly, with significantly stronger ESR intensities, the Al signal naturally tends to return a higher measurement precision compared to the Ti-mix and Ti-H signal (Duval et al., 2024). The same applies here. For example, at $t$ = 6.89 days after irradiation, the Al, Ti-mix and Ti-H signal intensities show a scatter of 1.9 %, 3.1 % and 4.6 %, respectively (Table 1). For BG03-06, at $t$ = 7.02 days, this variability is 2.9 % for the Al signal, while it is 5.3–5.4 % for both Ti signals. Importantly, these values are similar to those typically reported about the stability of the experimental setup (Duval et al., 2024; Duval and Guilarte Moreno, 2012).

Fig. 2 displays the spectra of the Al and Ti signals acquired at measurements #3, #33 and #63 for sample BG03-06. The Al spectra show little variability, with a slight shift of less than 1 Gauss (G) in the position of the first peak. A comparison of the ESR spectra obtained 7 days after gamma-irradiation with those acquired immediately after irradiation shows no significant differences for either Al or Ti signals. The small variations in peak intensity observed for Ti-mix or Ti-H are mostly attributable to high-frequency background noise, which is expected given the smaller $S/N$ measured for these signals compared to Al. It is worth noting that other studies have reported changes in signal shape between spectra recorded immediately after irradiation and after preheating (e.g., Prince et al., 2024). However, such effects were not observed in our experiments, as the samples were not preheated. A slight difference in peak amplitude was observed, for example around 3500 G and 3525 G, which we initially attributed to the angular dependence of the signal. Nevertheless, as highlighted in Fig. 2 for measurement #63, the Ti-mix (signal D) exhibits a higher ESR intensity around 3525 G, while the Ti-H signal remains unchanged. This suggests that the observed variation is more likely related to the Ti-Li component rather than to angular dependence alone.

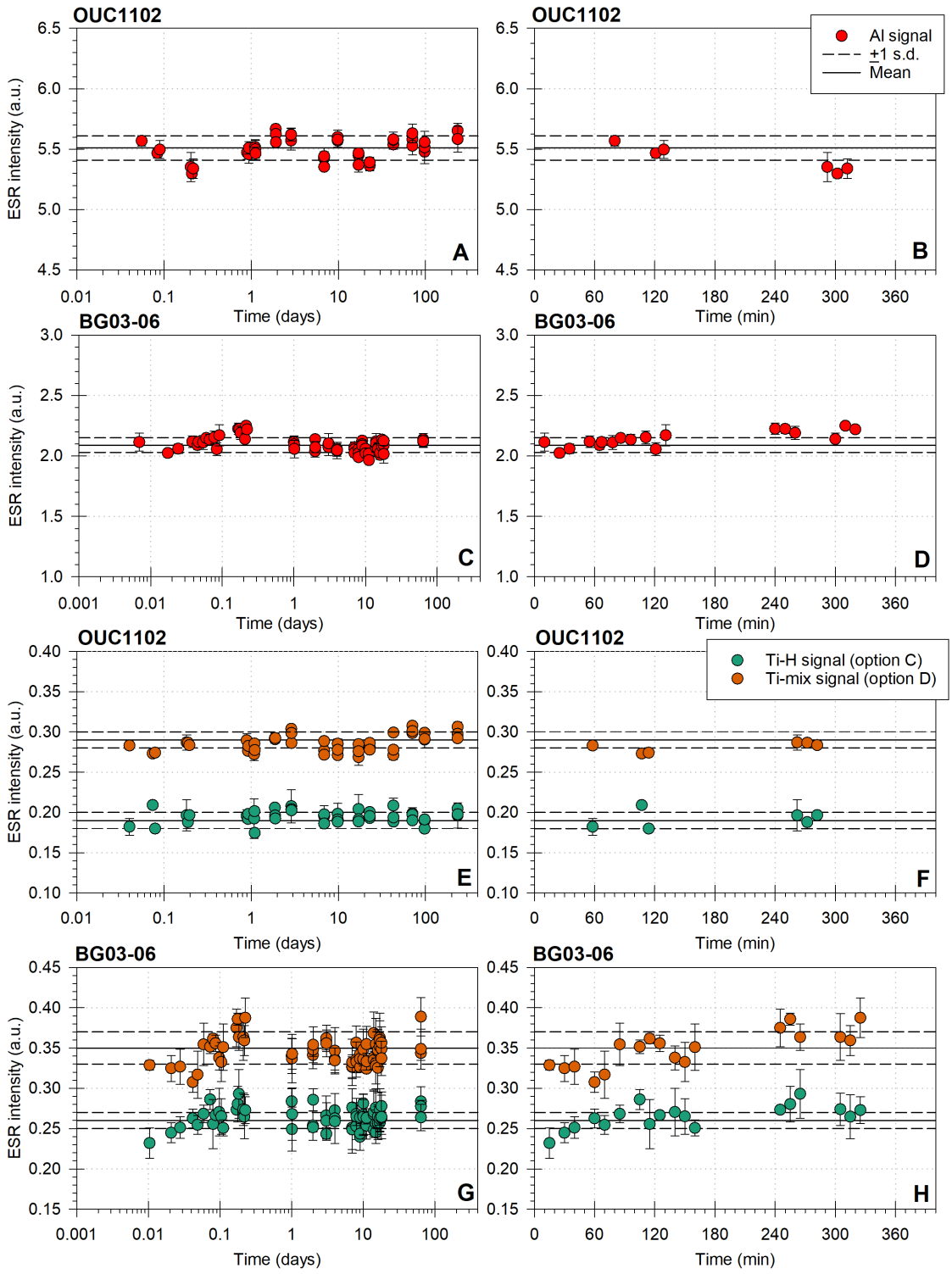


Figure 1: Evolution of the ESR intensities measured for the Al and Ti (options C and D sensu Duval and Guilarte, 2015) signals over almost 8 months (234 days) and 2 months (64 days) for samples OUC1102 and BG03-06, respectively. Left graphs (A, C, E, G) show the full evolution of the intensities over the full-time range. Right graphs (B, D, F, H) are focused on the first 400 minutes ($\sim$ 8 hours) after the irradiation. Graphs A to D show the Al signal, while graphs E to H display the Ti signals. Each point represents the mean ESR intensity and associated 1 standard deviation (s.d.) from the three measurements performed after a $\sim 120\,^{\circ}$ rotation. The mean ESR intensity (in arbitrary units – a.u.) and associated 1 sd over the full time range is also indicated by solid and dashed lines, respectively. All numerical values may be found in Supplementary Material Tables S1 and S2.

| | | Al signal | | | Ti-H signal option C sensu Duval and Guilarte (2015) | | | Ti-mix signal option D sensu Duval and Guilarte (2015) | | |
|---|---|---|---|---|---|---|---|---|---|---|
| **Sample** | *n* | **Duration after irradiation [min/day]** | **Mean ESR intensity ± 1 sd (cv)** | **Average** $S/N$ | **Duration after irradiation [min/day]** | **Mean ESR intensity ± 1 sd (cv)** | **Average** $S/N$ | **Duration after irradiation [min/day]** | **Mean ESR intensity ± 1 sd (cv)** | **Average** $S/N$ |
| OUC1102 | 3 | 129/0.09 | 5.51 ± 0.05 (1.7 %) | 193 | 114/0.08 | 0.19 ± 0.02 (8.5 %) | 12 | 114/0.08 | 0.28 ± 0.01 (2.0 %) | 24 |
| | 9 | 1362/0.95 | 5.44 ± 0.09 (1.7 %) | 145 | 1339/0.93 | 0.19 ± 0.01 (4.6 %) | 15 | 1339/0.93 | 0.28 ± 0.01 (2.1 %) | 28 |
| | 15 | 2775/1.93 | 5.49 ± 0.10 (1.8 %) | 167 | 2728/1.89 | 0.19 ± 0.01 (4.8 %) | 14 | 2728/1.89 | 0.28 ± 0.01 (2.5 %) | 27 |
| | 21 | 9919/6.89 | 5.49 ± 0.10 (1.9 %) | 163 | 9919/6.89 | 0.19 ± 0.01 (4.6 %) | 14 | 9919/6.89 | 0.28 ± 0.01 (3.1 %) | 29 |
| | 42 | 336889/234 | 5.51 ± 0.10 (1.7 %) | 149 | 336913/234 | 0.19 ± 0.01 (4.0 %) | 15 | 336913/234 | 0.29 ± 0.01 (3.6 %) | 29 |
| BG03-06 | 11 | 121/0.08 | 2.10 ± 0.04 (1.9 %) | 45 | 125/0.09 | 0.26 ± 0.02 (6.0 %) | 10 | 125/0.09 | 0.34 ± 0.02 (5.8 %) | 12 |
| | 21 | 1460/1.01 | 2.13 ± 0.06 (2.9 %) | 50 | 1465/1.02 | 0.27 ± 0.01 (5.6 %) | 10 | 1465/1.02 | 0.35 ± 0.02 (6.1 %) | 13 |
| | 33 | 10115/7.02 | 2.11 ± 0.06 (2.9 %) | 42 | 10120/7.03 | 0.26 ± 0.01 (5.3 %) | 14 | 10120/7.03 | 0.35 ± 0.02 (5.4 %) | 17 |
| | 48 | 20175/14.01 | 2.09 ± 0.06 (3.0 %) | 48 | 20230/14.05 | 0.26 ± 0.01 (4.5 %) | 14 | 20230/14.05 | 0.34 ± 0.02 (4.9 %) | 18 |
| | 63 | 92180/64.01 | 2.09 ± 0.06 (2.9 %) | 54 | 92180/64.01 | 0.26 ± 0.01 (4.3 %) | 15 | 92180/64.01 | 0.35 ± 0.02 (4.8 %) | 20 |

Table 1: Mean ESR intensities and associated standard deviation measured for the Al, Ti-H (option C) and Ti-mix (option D) signals for a given duration, i.e., after about 2 hours, 1 day, 2 days, 1 week (7 days), and almost 8 months (234 days) for OUC1102, and after about 2 hours, 1 day, 1 week (7 days), 2 weeks (14 days) and about 2 months (64 days) for BG03-06. Key: $n$ = measurement number; sd = standard deviation; cv = coefficient of variation. The average $S/N$ (signal-to-noise ratio) has been calculated by averaging the noise at times 3, 9, 15, 21, 42 for sample OUC1102 and at times 11, 21, 33, 48 and 63 for sample BG03-06. All data, uncorrected and corrected with the standard are provided in the Supplementary Material.

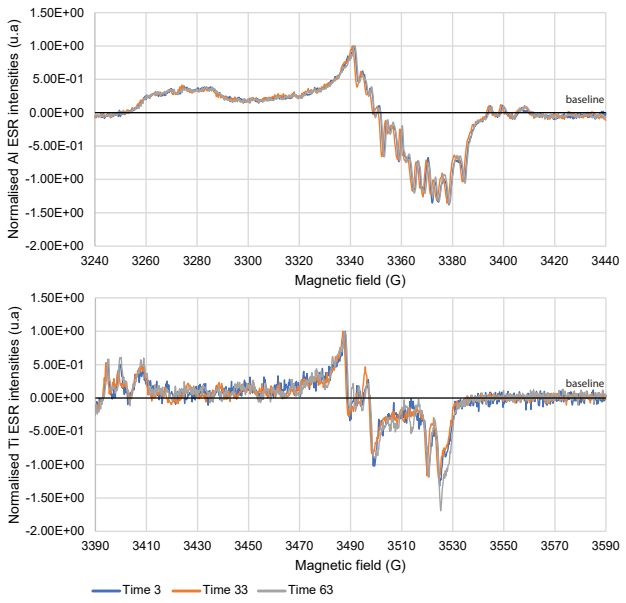


Figure 2: Comparison of normalised Al and Ti signals of sample BG03-06 from measurements #3, #33 and #63. A baseline correction using a cubic function was applied for each spectrum.

## 4. Summary

Our main observations may be summarised as follows:

- No apparent systematic trend in the short-term ESR signals stability is observed over time: while OUC1102 shows either a slight decrease (Al signal) or remains somewhat stable (Ti signals) during the first hours after gamma-irradiation, an intensity increase may instead be observed for all signals of BG03-06 over that same period.

- In other words, the more pronounced trends observed during the first day after gamma-irradiation are strongly signal- and sample-dependent. The intensity corrections performed using a standard measured together with the sample enable minimising the influence of the relative instability of the experimental setup on the data set, ensuring that the observed trends primarily reflect sample-specific behavior.

- Mean ESR intensities remain within error independently of the time range considered: over 2 hours, 1 day, 2 days or 7 seven days after gamma irradiation, the mean ESR intensity is consistent with the baseline value obtained over several months of measurements. This simply indicates that the ESR intensities measured shortly after gamma-irradiation do not significantly differ from the mean values derived from a longer time range.

## 5. Conclusions

Our results indicate that Al and Ti signals measured in two quartz samples do not exhibit on average any significant change in their intensity shortly (2 hours, 1 day, 2 days or even 7 days) after gamma-irradiation, suggesting that the transient radiation-induced signals, if present, have negligible influence on the measured ESR intensities. In other words, any potential transient signal generated immediately following the irradiation falls within the intrinsic experimental uncertainty, which is largely driven by factors such as the stability of the ESR spectrometer, the inherent heterogeneity of the quartz sample, or the $S/N$ ratio. While some apparent trends may be punctually observed during the first 5 hours or 1 day after gamma-irradiation, they may be sample dependent and are possibly related to the stability of the ESR spectrometer, although the influence of the latter was tentatively minimised by repeatedly measuring a quartz standard. For precaution, it may nevertheless be recommended to wait at least 1 day after gamma-irradiation before performing the ESR measurements. An extension of the current study could involve preheating the gamma-irradiated samples followed by the same set of measurements.

Notably, our observations are consistent with those of Tsukamoto et al. (2015), who showed that Al and Ti centres remain stable over time following X-ray irradiation, with no significant differences between signals regenerated immediately after irradiation and those measured after one month of storage. Taken together, their findings and ours support the conclusion that potential short-lived components have little to no impact on ESR signal stability. As a corollary, these results also indicate that there is currently no evidence of short-term fading of the Al and Ti signals measured in quartz. As a consequence, this study provides an important experimental foundation for the future development and broader application of time-efficient Single Aliquot Regenerative dose (SAR) protocols using gamma-irradiation sources. Such advancement could significantly streamline the ESR dating workflow, particularly in contexts where sample quantity is limited or rapid turnaround is required.

**Data availability.** All data acquired in this study are available as Supplementary Material to this article.

**Conflict of interest.** The authors declare that they have no conflict of interest that could have biased their scientific work.

**Financial support.** EBA's postdoctoral research has received funding from the European Union's Horizon 2020 research and innovation programme under the Marie Skłodowska-Curie grant agreement No 101107408. MD's investigation is supported by the Spanish Ramón y Cajal Fellowship RYC2018-025221-I funded by MCIN/AEI/10.13039/501100011033 and by "ESF Investing in your future", and Grants PALEOMED PID2021-123092NB-C22 and GBCHRON PID2024-155126NB-I00, both funded by

MICIU/AEI/10.13039/501100011033 and by ERDF/EU.

**Review.** This article was reviewed by an anonymous reviewer.

## References

Bartz, M., Arnold, L.J., Demuro, M., Duval, M., King, G.E., Rixhon, G., Álvarez Posada, C., Parés, J.M., Brückner, H., 2019. Single-grain TT-OSL dating results confirm an Early Pleistocene age for the lower Moulouya River deposits (NE Morocco). Quaternary Geochronology 49, 138–145. doi: 10.1016/J.QUAGEO.2018.04.007.

Bartz, M., Rixhon, G., Duval, M., King, G.E., Álvarez Posada, C., Parés, J.M., Brückner, H., 2018. Successful combination of electron spin resonance, luminescence and palaeomagnetic dating methods allows reconstruction of the Pleistocene evolution of the lower Moulouya river (NE Morocco). Quaternary Science Reviews 185, 153–171. doi: 10.1016/J.QUASCIREV.2017.11.008.

Ben Arous, E., Blinkhorn, J.A., Elliott, S., Kiahtipes, C., N'Zi, C., Bateman, M.D., Duval, M., Roberts, P., Patalano, R., Blackwood, A., Niang, K., Kouamé, E., Lebato, E., Hallett, E., Cerasoni, J.N., Scott, E., Lgner, J., Escarza, M.J.A., Guédé, F.Y., Scerri, E.M.L., 2025. Humans in Africa's wet tropical forests 150 thousand years ago. Nature 640, 402–407. doi: 10.1038/s41586-025-08613-y.

Ben Arous, E., Duttine, M., Duval, M., 2024a. How to measure the ESR intensity of the Al centre in optically bleached coarse quartz grains for dating purpose? Radiation Physics and Chemistry 214, 111307. doi: 10.1016/J.RADPHYSCHEM.2023.111307.

Ben Arous, E., Niang, K., Blinkhorn, J.A., Del Val, M., Medialdea, A., Coussot, C., Alonso Escarza, M.J., Bateman, M.D., Churruca Clemente, A., Blackwood, A.F., Iglesias-Cibanal, J., Saíz, C., Scerri, E.M.L., Duval, M., 2024b. Constraining the age of the Middle Stone Age locality of Bargny sites (Senegal) through a combined OSL-ESR dating approach. Quaternary Environments and Humans doi: 10.1016/j.qeh.2024.100044.

Duval, M., Arnold, L.J., Demuro, M., Parés, J.M., Campaña, I., Carbonell, E., Bermúdez de Castro, J.M., 2022. New chronological constraints for the lowermost stratigraphic unit of Atapuerca Gran Dolina (Burgos, N Spain). Quaternary Geochronology 71, 101292. doi: 10.1016/j.quageo.2022.101292.

Duval, M., Arnold, L.J., Guilarte, V., Demuro, M., Santonja, M., Pérez-González, A., 2017. Electron spin resonance dating of optically bleached quartz grains from the Middle Palaeolithic site of Cuesta de la Bajada (Spain) using the multiple centres approach. Quaternary Geochronology 37, 82–96. doi: 10.1016/j.quageo.2016.09.006.

Duval, M., Guilarte, V., 2015. ESR dosimetry of optically bleached quartz grains extracted from Plio-Quaternary sediment: Evaluating some key aspects of the ESR signals associated to the Ti-centers. Radiation Measurements 78, 28–41. doi: 10.1016/j.radmeas.2014.10.002.

Duval, M., Guilarte, V., Bartz, M., Alonso Escarza, M.J., Ben Arous, E., del Val, M., García Rodríguez, C., 2024. ESR dating of optically-bleached quartz grains: Evaluating measurement repeatability and reproducibility. Radiation Physics and Chemistry 215, 111313. doi: 10.1016/j.radphyschem.2023.111313.

Duval, M., Guilarte Moreno, V., 2012. Assessing the influence of the cavity temperature on the ESR signal of the Aluminum center in quartz grains extracted from sediment. Ancient TL 30, 11–16. doi: 10.26034/la.atl.2012.463.

Fattibene, P., Callens, F., 2010. EPR dosimetry with tooth enamel: A review. Applied Radiation and Isotopes 68, 2033–2116. doi: 10.1016/J.APRADISO.2010.05.016.

Guilarte, V., Duval, M., 2020. ESR dating of optically bleached quartz grains: Assessing the impact of different experimental setups on dose evaluations. Geochronometria 48, 179–190. doi: 10.2478/geochr-2020-0005.

Hoffmann, D., Mangini, A., 2002. Comparative studies on the $CO_2$-signal in tooth enamel and carbonates. Radiation Protection Dosimetry 101, 359–362. doi: 10.1093/OXFORDJOURNALS.RPD.A006001.

IAEA, 2002. Use of the Electron Paramagnetic Resonance Dosimetry with Tooth Enamel for Retrospective Dose Assessment. IAEA-TECDOC-1331. International Atomic Energy Agency, Austria , 57.

Liu, C.R., Yin, G.M., Gao, L., Bahain, J.J., Li, J.P., Lin, M., Chen, S.M., 2010. ESR dating of Pleistocene archaeological localities of the Nihewan Basin, North China – Preliminary results. Quaternary Geochronology 5, 385–390. doi: 10.1016/J.QUAGEO.2009.05.006.

Nilsson, J., Lund, E., Lund, A., 2001. The effects of UV-irradiation on the ESR-dosimetry of tooth enamel. Applied Radiation and Isotopes 54, 131–139. doi: 10.1016/S0969-8043(99)00275-4.

Niu, Y., Fan, Y., Qiao, Y., Lü, T., Li, C., Qi, L., Wang, S., Peng, S., Tan, Y., 2022. Chronostratigraphy of a loess-paleosol sequence in the western Chinese Loess Plateau based on ESR dating and magnetostratigraphy. Quaternary International 637, 1–11. doi: 10.1016/J.QUAINT.2022.08.005.

Prince, E., Tsukamoto, S., Grützner, C., Vrabec, M., Ustaszewski, K., 2024. Not too old to rock: ESR and OSL dating reveal Quaternary activity of the Periadriatic Fault in the Alps. Earth, Planets and Space 76, 1–27. doi: 10.1186/S40623-024-02015-6.

Sala-Ramos, R., Chacón, M.G., Aouraghe, H., Haddoumi, H., Morales, J.I., Rodríguez-Hidalgo, A., Tornero, C., Oujaa, A., Soto, M., Farkouch, M., Aissa, E.M., El Atmani, A., Duval, M., Arnold, L.J., Demuro, M., Blain, H.A., Piñero, P., Rivals, F., Burjachs, F., Tarriño, A., Álvarez-Posada, C., Souhir, M., Saladié, P., Pla-Pueyo, S., Larrasoña, J.C., Marín, J., Moreno, E., De Lombera-Hermida, A., Bartrolí, R., Lombao, D., García-Argudo, G., Ramírez, I., Díez-Canseco, C., Tomasso, S., Expósito, I., Allué, E., Noureddine, H., Mhamdi, H., Rhosne, H., Carrancho, A., Villalaín, J.J., Van der Made, J., Canals, A., Benito, A., Agustí, J., Parés, J.M., 2022. Evolución del asentamiento humano en la región de Aïn Beni Mathar – Guefaït (Jerada, Marruecos Oriental). Takurunna 10–11, 179–203.

Sholom, S., Chumak, V., 2008. Age-related peculiarities of tooth enamel as a natural EPR biodosimeter. Radiation Measurements 43, 823–826. doi: 10.1016/J.RADMEAS.2007.11.058.

Toyoda, S., Falguères, C., 2003. The method to represent the ESR signal intensity of the aluminium hole center in quartz for the purpose of dating. Advances in ESR Applications 20, 7–10.

Tsukamoto, S., Toyoda, S., Tani, A., Oppermann, F., 2015. Single aliquot regenerative dose method for ESR dating using X-ray irradiation and preheat. Radiation Measurements 81, 9–15. doi: 10.1016/J.RADMEAS.2015.01.018.

Voinchet, P., Pereira, A., Nomade, S., Falguères, C., Biddittu, I., Piperno, M., Moncel, M.H., Bahain, J.J., 2020. ESR dating applied to optically bleached quartz - A comparison with $^{40}Ar/^{39}Ar$ chronologies on Italian Middle Pleistocene sequences. Quaternary International 556, 113–123. doi: 10.1016/j.quaint.2020.03.012.

Yokoyama, Y., Falguères, C., Quaegebeur, J.P., 1985. ESR dating of quartz from Quaternary sediments: first attempts. Nuclear Tracks 10, 921–928. doi: 10.1016/0735-245X(85)90109-7.